NASA TECHNICAL MEMORANDUM 89100

A PARAMETRIC STUDY OF FRACTURE TOUGHNESS OF FIBROUS COMPOSITE MATERIALS

C. C. POE, JR.

FEBRUARY 1987

NASA
National Aeronautics and
Space Administration

Langley Research Center
Hampton, Virginia 23665

INTRODUCTION

Fibrous composite materials can be as strong and stiff as steel, have a lower density than magnesium, and can be tailored to have maximum strength and stiffness in specific directions. The weight saving potential of composites is well documented. Simple structural members such as beams and pipes can be made with relatively inexpensive processes such as pultrusion, braiding, and filament winding. Larger structures can be made using filament winding and automatic tape laying machines. These processes are not labor intensive and produce structures with relatively few parts. Thus, composite structures have the potential to be cost effective and even cheaper in some cases. On the other hand, composites are very notch sensitive because of the linear-elastic fibers that carry most, if not all, of the load.

Composites do not develop through-the-thickness fatigue cracks as do metals. However, low-velocity impacts caused by debris, dropped tools, and collisions can break fibers resulting in crack-like damage and a reduction in tension strength [1,2]. The damage can extend completely through the thickness or part way through the thickness of thick laminates. Thus, fracture toughness is a very important property of composites as well as metals.

The fracture toughness of composites depends on fiber and matrix properties, fiber orientations, and stacking sequence. There are far too many combinations of fiber, matrix, and layup to evaluate experimentally. Thus, some analytical guidance is needed to select fiber, matrix, and layup to give maximum fracture toughness for a given strength and stiffness. Accordingly, a parametric study was made to determine how fracture toughness is affected by fiber and matrix properties and fiber orientations. Stacking sequence, which affects interlaminar stresses and bending stiffness, was not studied. The laminates were assumed to be balanced (equal number of plies with $+\alpha$ and $-\alpha$ orientations) and, except for a filament wound laminate, symmetric about the midplane. Otherwise, bending and twisting could accompany stretching. Comparisons were made with test data for through-the-thickness cracks and surface cracks to give credibility to the study. Both $[0^\circ_i/\pm 45^\circ_j/90^\circ_k]_{ns}$ and $[0^\circ_i/\pm\alpha_j]_{ns}$ laminates with resin matrices were considered. These include most laminates of interest. The general fracture toughness parameter developed in [3] and [4] was used to predict the fracture toughness. This method only required the elastic constants of the laminae, the fiber failing strain, and the fiber orientations. These properties are readily obtainable.

NOMENCLATURE

a	surface cut depth, m
c	half-length of surface cut and through-the-thickness cut, m
d_o	value of r for $\epsilon_{1c} = \epsilon_{tuf}$

E	Young's modulus, Pa
F_{tu}	ultimate tensile strength of laminate (unnotched), Pa
F_{tuf}	ultimate tensile strength of fibers, Pa
G	shear modulus, Pa
K_Q	fracture toughness, $Pa\sqrt{m}$
K_{Qe}	elastic fracture toughness, $Pa\sqrt{m}$
n	number of repeating ply groups
N_o	half the number of plies in a quasi-isotropic laminate
Q	shape factor for an elliptical crack
Q_c	critical value of the general fracture toughness parameter, $\sqrt{m}$
r	distance from the crack tip (along the y-axis), m
S_c	gross failing stress for laminates with through-the-thickness cuts and gross stress for failure of first ligament in laminates with surface cuts, Pa
S_r	gross stress for failure of remaining ligament in laminates with surface cuts, Pa
t	laminate thickness, m
t_{min}	minimum laminate thickness for two-part failure with surface cuts, m
V_f	fiber volume fraction
W	width of specimen in test section, m
α	ply orientation angle (relative to loading axis)
α^*	orientation angle of principal load-carrying plies
ϵ_{lc}	principal strain distribution in principal load-carrying plies at failure
ϵ_{tuf}	ultimate tensile failing strain of the fibers

ϕ parametric angle of ellipse ($\phi = 0^\circ$ - bottom of surface cut and $\phi = 90^\circ$ - top of surface cut)

ν Poisson's ratio

Subscripts:

i,j,k half the number of 0°, $\pm 45^\circ$ or $\pm\alpha^\circ$, and 90° plies

x,y Cartesian coordinates (The y-direction corresponds to the axial loading direction of the specimen or laminate.)

1,2 principal ply coordinates (1 refers to fiber direction)

The following notation is used to describe layup. All laminates are symmetric about the midplane as indicated by the lower case "s" outside the parentheses. Fiber angles are separated by a slash and listed in the order of layup from the outside to the midplane. A numerical subscript on the fiber angle denotes how many consecutive plies are at that angle. Likewise, a numerical subscript on a group of plies denotes how many consecutive groups have that pattern.

PREDICTIONS OF FRACTURE TOUGHNESS

In [3] and [4], a general fracture toughness parameter that is a constant for all fibrous composite materials was derived. This parameter can be used to predict the fracture toughness of composite laminates using only the elastic constants of the laminate E_x, E_y, and ν_{yx} and the ultimate tensile failing strain of the fibers ϵ_{tuf}. The predictions were tested for both metal and resin matrices with boron, graphite, or glass fibers. The derivation is briefly repeated below.

First, attention was directed to the principal load-carrying plies. These plies are usually the ones most aligned with the loading direction and hence carry most of the axial load. Consequently, their failure is sufficient to cause the failure of all other plies. Here, the 0° plies are the principal load-carrying plies. See figure 1. Of course, the principal load-carrying plies would have some other orientation if there were no 0° plies. For example, in $[\pm 45^\circ]_{ns}$ or $[\pm 30^\circ_j/90^\circ_k]_{ns}$ laminates, the principal load-carrying plies are the $\pm 45^\circ$ and $\pm 30^\circ$ plies, respectively.

Next, failure of the principal load-carrying plies was predicted by using a maximum-strain criterion. At failure, the fiber strains ahead of a crack tip in a specially orthotropic laminate under plane stress and mode I conditions are given by

$$\epsilon_{1c} = Q_c(2\pi r)^{-1/2} + B_o + B_1 r^{1/2} + B_2 r^{3/2} + \ldots \quad (1)$$

where r is the distance from the crack tip. The coefficient Q_c is the general fracture toughness parameter given by

$$Q_c = \frac{K_Q \xi}{E_y} \quad (2)$$

and

$$\xi = [1 - \frac{\nu_{yx} E_x^{1/2}}{E_y^{1/2}}][\frac{E_y^{1/2} \sin^2 \alpha^*}{E_x^{1/2}} + \cos^2 \alpha^*]$$

The angle α^* is the angle that the principal load-carrying fibers make with the y-axis.

At failure, the critical level of fiber strains in the principal load-carrying plies just ahead of the crack tip was assumed to be the same for any layup. Furthermore, the critical strain level was assumed to increase in proportion to the ultimate tensile failing strain of the fibers ϵ_{tuf}. This criterion is equivalent to a point-strain criterion applied to the principal load-carrying plies. That is, at failure, $\epsilon_{1c} = \epsilon_{tuf}$ at $r = d_o$ in equation (1). By retaining only the $r^{-1/2}$ term, equation (1) gives

$$\frac{Q_c}{\epsilon_{tuf}} = (2\pi d_o)^{1/2}$$

which is a constant for all composite laminates, independent of layup and material.

Values of Q_c/ϵ_{tuf} were calculated from the strengths of composite specimens containing central crack-like cuts that extended through the thickness [4]. The composite laminates had various layups and were made of resin and metal matrix materials with graphite, boron, and glass fibers. The thickest of the laminates had 16 plies. A representative value of Q_c/ϵ_{tuf} was 1.5 $\sqrt{mm}$ (d_o = 0.36 mm). Replacing Q_c by $1.5\epsilon_{tuf}\sqrt{mm}$ in equation (2) and solving for K_Q gives

$$K_Q = \frac{1.5\epsilon_{tuf} E_y}{\xi} \quad (3)$$

The value of E_y/ξ in equation (3) can be calculated from lamina constants using lamination theory. Thus, only lamina constants and ϵ_{tuf} of the fibers are

required to predict the fracture toughness. The lamina constants and values of ϵ_{tuf} used in this paper are given in table I.

Table I.- Lamina properties.

Material	E_{11}, GPa	E_{22}, GPa	G_{12}, GPa	ν_{12}	F_{tuf}, GPa	ϵ_{tuf}	V_f
T300/5208	129.	10.9	5.65	0.312	2.20	0.0100	0.63
T300/BP-907	109.	8.32	4.82	.314	2.20	.0100	.54
Celion 6000/ .... polyimide	136.	9.31	6.14	.357	2.20	.0100	.61
AS4/HBRF-55	-	-	-	-	-	-	.54
0° plies	106.	6.39	4.47	.275	2.43	.0124	
$\pm 56.5^\circ$ plies .	111.	1.92	4.28	.267	-	-	
Boron/epoxy	207.	20.7	7.31	.270	3.50	.0075	.45
Kevlar-49/epoxy .	74.1	5.16	2.07	.421	2.15	.0165	.6
E-Glass/epoxy ...	38.6	8.27	4.14	.260	1.40	.0200	.53
S-Glass/epoxy	49.4	17.8	4.48	.291	2.08	.0271	.6

The 0° plies in some of the resin matrix laminates in [4] split at the ends of the cuts and delaminated before the laminates failed. Splits and delaminations are not taken into account in equations (1) and (2). Long splits accompanied by delaminations can greatly reduce the stress concentration factor [5] and hence elevate the strengths and values of Q_c/ϵ_{tuf} calculated with equation (2). Therefore, the values of Q_c/ϵ_{tuf} that were calculated for laminates with large splits and delaminations in [4] were not valid. These laminates had 50 percent or more 0° plies or several consecutive 0° plies. The matrix failures resulted from the low transverse normal strength and shear strength of the 0° plies and the large interlaminar stresses between the 0° and $\pm\alpha$ plies. The 1.5 $\sqrt{mm}$ value for Q_c/ϵ_{tuf} from [4] is an average of the values for laminates where the splits and delaminations were judged to be small compared to the length of the cut, much like plastic zone sizes in metals.

An experimental investigation of Harris and Morris [6,7] showed that the effect of splits and delaminations at the ends of the cut depends on the thickness of the laminate. They tested center-cracked, compact, and three-point-bend specimens made from $[0^\circ/\pm 45^\circ/90^\circ]_{ns}$, $[0^\circ/\pm 45^\circ]_{ns}$, and $[0^\circ/90^\circ]_{ns}$ T300/5208 laminates. The average values for K_Q from the center-cracked specimens are plotted in figure 2 against the number of ply groups 2n. They were calculated using

$$K_Q = K_{Qe}\left(1 - \frac{c_o K_{Qe}^2}{c K_Q^2}\right)^{-1} \qquad (4)$$

where

$$K_{Qe} = S_c(\pi c \sec \frac{\pi c}{W})$$

and

$$c_o = \frac{K_Q^2}{\pi F_{tu}^2}$$

Equation (4) was derived assuming the existence of an initial flaw of length $2c_o$ such that the actual length of the cut is $2(c + c_o)$ and that $S_c = F_{tu}$ for $c = 0$. The vertical lines were drawn through the symbols to indicate the dispersion. Values for K_Q predicted with equation (3) are also plotted. The values for $[0^\circ/\pm45^\circ/90^\circ]_{ns}$ and $[0^\circ/90^\circ]_{ns}$ are equal. (More is said about layups with equal K_Q subsequently.) The test values for K_Q for $[0^\circ/\pm45^\circ/90^\circ]_{ns}$ and $[0^\circ/90^\circ]_{ns}$ decrease initially with increasing thickness and those for $[0^\circ/\pm45^\circ]_{ns}$ increase. With increasing thickness, the values asymptotically approach within 10 percent of the predicted values.

Using pyrolysis, Harris and Morris [6,7] separated the plies of specimens (deplied) that had been loaded to within a few percent of their estimated strength. Matrix and fiber damage in individual plies was then visible. They found that splits and delaminations at the ends of the cuts were confined to the plies near the surfaces, similar to edge delaminations in thick laminates [8]. However, 0° fibers were broken in the interior plies for a short distance ahead of the cut. The surface plies carry a large portion of the load in thin laminates but not in thick laminates. Thus, the splits and delaminations dominated the fracture of thin laminates but not the fracture of thick laminates. As noted previously, the 0° splits and delaminations tend to elevate strengths and fracture toughness as evidenced by the thin $[0^\circ/\pm45^\circ/90^\circ]_{ns}$ and $[0^\circ/90^\circ]_{ns}$ specimens. The initial increase of fracture toughness with thickness was unexpected for the $[0^\circ/\pm45^\circ]_{ns}$ specimens. The $\pm45^\circ$ fibers in the thin $[0^\circ/\pm45^\circ/90^\circ]_{ns}$ and $[0^\circ/90^\circ]_{ns}$ specimens broke ahead of the cut, more or less, but not those in the thin $[0^\circ/\pm45^\circ]_{ns}$

specimens. Instead, the $\pm 45^\circ$ plies delaminated prematurely throughout the net section, apparently reducing strengths and toughnesses.

Equation (3) should be valid for other T300/5208 laminates with similar proportions of 0° plies and with more than 10 to 20 ply groups as long as many 0° plies are not grouped together. It is probably valid for T300/5208 laminates with more than 50 percent 0° plies (the maximum proportion in figure 2) but certainly not for as many as 100 percent. Unidirectional graphite/epoxy laminates (all 0° plies) tend to split at the ends of a cut regardless of thickness. It is important to realize that equation (3) can give accurate predictions for resin-matrix laminates thinner than 10 to 20 ply groups as evidenced by the results in [4]. Even the predictions in figure 2 for $[0^\circ/\pm 45^\circ/90^\circ]_{ns}$ and $[0^\circ/\pm 45^\circ]_{ns}$ T300/5208 laminates are reasonably accurate for thin laminates. The amount of splitting and delaminating depends on the fiber and matrix properties as well as layup. Stronger fibers result in higher matrix stresses and more splitting and delaminating, whereas stronger matrices result in less splitting and delaminating. Thus, the range of applicability of equation (3) depends on the properties of the fibers and matrix as well as the layup.

PARAMETRIC STUDY OF FRACTURE TOUGHNESS

Fiber Properties

Many people incorrectly associate high fracture toughness of composites with high failing strain of the fibers. For quasi-isotropic laminates, which have $E_x = E_y$, equation (3) can be written in terms of lamina constants as

$$K_Q = 0.75 V_f F_{tuf} \frac{\left[1 + \dfrac{E_{22}(1 + 2\nu_{12})}{E_{11}}\right]}{(1 - \nu_{12})} \tag{5}$$

where $E_{11}\epsilon_{tuf}$ was replaced with $V_f F_{tuf}$. Thus, fracture toughness increases in proportion to fiber strength, not failing strain, and fiber volume fraction. Expressing equation (5) as a series, one can show that K_Q increases in proportion to $V_f F_{tuf}(1 + E_{22}/E_{11} + \nu_{12} + \ldots)$. Thus, E_{11}, E_{22}, and ν_{12} have less effect on K_Q than V_f and F_{tuf}. Similar results can be shown for other layups.

Test values for K_Q from [4] were divided by fiber volume fraction V_f and plotted against fiber strength F_{tuf} in figure 3 for $[0^\circ/\pm 45^\circ/90^\circ]_{ns}$ laminates made with five different combinations of fiber and resin matrix materials. All the laminates were relatively thin: for boron/epoxy, $n = 1$,

otherwise, $n = 2$. Also, values for K_Q/V_f from equation (5) are plotted for $E_{22}/E_{11} = 0$, 0.1, and 0.2 with $\nu_{12} = 0.3$. For the boron and graphite laminates, $.07 < E_{22}/E_{11} < .1$, and for the E-glass/epoxy laminate, $E_{22}/E_{11} = .2$. The test values for K_Q/V_f agree well with the appropriate curves from equation (5). Notice that the laminate with the smallest fiber failing strain (shown in parentheses) has the largest fracture toughness and vice versa.

The ratio of strength with crack-like damage to undamaged strength, S_c/F_{tu}, is a measure of notch sensitivity. Materials with large values of S_c/F_{tu} are notch insensitive, whereas materials with small values of S_c/F_{tu} are notch sensitive. Solving equation (4) for S_c/F_{tu}, gives

$$\frac{S_c}{F_{tu}} = \frac{K_Q}{F_{tu}[\pi(c + c_o)]^{1/2}} \tag{6}$$

Thus, for a given crack size, the relative amount of strength retained increases in proportion to K_Q/F_{tu}. Dividing equation (3) by F_{tu} and replacing $\epsilon_{tuf}E_y$ by F_{tu}, gives

$$\frac{K_Q}{F_{tu}} = \frac{1.5}{\xi} \tag{7}$$

and substituting equation (7) into (6) gives

$$\frac{S_c}{F_{tu}} = \frac{1.5K_Q}{\xi[\pi(c + c_o)]^{1/2}} \tag{8}$$

Thus, for composite laminates, the relative amount of strength retained varies inversely with ξ. The right-hand side of equation (8) cannot be written in a simple expression of lamina constants for all laminates with $E_x = E_y$ like equation (5). However, for quasi-isotropic laminates, which are a subset of those with $E_x = E_y$, one can show that

$$\frac{K_Q}{F_{tu}} = 0.75\frac{[3(1 + \frac{E_{22}}{E_{11}}) + \frac{2\nu_{12}E_{22}}{E_{11}} + \frac{4G_{12}}{E_{11}}(1 - \frac{\nu_{12}^2E_{22}}{E_{11}})]}{[1 + \frac{E_{22}}{E_{11}} - \frac{2\nu_{12}E_{22}}{E_{11}} + \frac{4G_{12}}{E_{11}}(1 - \frac{\nu_{12}^2E_{22}}{E_{11}})]} \tag{9}$$

(Quasi-isotropic laminates with $2N_o$ plies have ply orientations of 0°, $180^\circ/N_o$, $360^\circ/N_o$, $(N_o - 1)180^\circ/N_o$ ..., where $N_o \geq 3$.) The right hand side of equation (9) depends only on fiber and matrix modulae. For $E_{22}/E_{11} = G_{12}/E_{11} = 0$, which represents the high-modulus fibers in table I, $K_Q/F_{tu} = 2.25\ \sqrt{mm}$. For the S-Glass/epoxy, which has the largest value for E_{22}/E_{11} in table I, $K_Q/F_{tu} = 2.32\ \sqrt{mm}$. Therefore, the notch sensitivity of quasi-isotropic laminates is virtually independent of fiber properties. Ultimate tensile strength also increases in proportion to fiber strength, much like fracture toughness in equation (5). Therefore, stronger fibers can be selected to increase ultimate tensile strength and decrease weight without increasing notch sensitivity. Similar results can be shown for other layups. On the other hand, fracture toughness and ultimate tensile strength of metals do not necessarily increase together, and metals with large ultimate tensile strengths are usually more notch sensitive than those with smaller ultimate tensile strengths.

Hybrids

When different fibers are combined to make a hybrid laminate, fracture toughness increases with increasing fiber modulus as well as increasing fiber strength. Test [9] and predicted values for fracture toughness are plotted in figure 4 for Kevlar-49/graphite/epoxy and S-glass/graphite/epoxy hybrid laminates. The layups are $[45^\circ/0^\circ/-45^\circ/90^\circ]_{2s}$, where the $\pm 45^\circ$ and 90° plies are T300 fibers and the 0° plies are Kevlar-49 or S-glass. These fibers have similar strengths, but the graphite fibers are much stiffer than the others. In all cases, the resin is 5208 epoxy. For comparison, predictions are shown for all-graphite, all-Kevlar-49, and all-S-glass.

Although the fiber strengths are nearly equal, the values for fracture toughness for the hybrids are considerably greater than those for the non-hybrids made from the same constituents. Thus, the combination of materials can increase fracture toughness synergistically. The basic reason for the increase in fracture toughness is that the graphite fibers are much stiffer than the S-glass and Kevlar-49 fibers, causing the $\pm 45^\circ$ plies in the hybrids to carry a greater share of the load. The S-glass fibers have the lowest modulus and result in the hybrid with the highest fracture toughness. Also, the fracture toughness of the all-S-glass is higher than the all-Kevlar-49 and all-graphite because the ratio E_{22}/E_{11} is larger. The test values are higher than predicted for the hybrids because of matrix damage at the ends of the cuts.

Matrix Properties

Equation (5) for quasi-isotropic laminates predicts the same fracture toughness for the same E_{22}/E_{11}, G_{12}/E_{11}, and ν_{12}. The T300 and Celion graphite fibers in table I have nearly the same strengths and failing strains,

however the 5208, BP-907, and polyimide matrices have quite different strengths and failing strains. For example, the strength and failing strain of BP-907 epoxy are about two times those of 5208 epoxy. Nevertheless, E_{22}/E_{11}, G_{12}/E_{11}, and ν_{12} are about the same for the T300 and Celion laminates, resulting in about the same values for K_Q/V_f. See figure 3.

Additional comparisons are made in figure 5 for $[45^\circ/0^\circ/-45^\circ/0^\circ]_{2s}$ laminates made with 5208 and BP-907 epoxies. The $[45^\circ/0^\circ/-45^\circ/90^\circ]_s$, $[45^\circ/0^\circ/-45^\circ/90^\circ]_{2s}$, are also included. The test values were reported in [10]. The fracture toughness values were normalized by fiber volume fractions, which are significantly lower for the BP-907 laminates than the 5208 laminates. For a given layup, the test values for BP-907 and 5208 are nearly equal as predicted. The difference between the tests and predictions is due to matrix damage at the ends of the cuts. Probably, the BP-907 values were a little lower than the 5208 values because the matrix damage was smaller for the BP-907 laminates than the 5208 laminates [10]. The test values for the $[45^\circ/0^\circ/-45^\circ/0^\circ]_{2s}$ laminates were lower than the predicted values, much like those for the $[0^\circ/\pm45^\circ]_{ns}$ T300/5208 laminates in figure 2. Perhaps this trend is peculiar to $[0^\circ_i/\pm45^\circ_j]_{ns}$ laminates. In summary, without significant matrix damage at the ends of the cuts or delaminations in the net section, the properties of resin matrices have little effect on fracture toughness.

The fracture toughness of laminates with aluminum and resin matrices cannot be compared directly because of the nonlinear compliance of laminates with aluminum matrices. However, strengths of $[0^\circ/\pm45^\circ]_s$, $[0^\circ/\pm45^\circ]_{2s}$, and $[0^\circ_2/\pm45^\circ]_s$ boron/aluminum and T300/5208 laminates with cuts (normalized by ultimate tensile strength) were compared in [4]. For a given proportion of 0° and 45° plies, the normalized strengths were about the same. Thus, as long as matrix damage at the ends of the cut is small and the fibers carry most of the load, even the differences between the properties of resin and metal matrices have little effect on fracture strengths, which is equivalent to little effect on fracture toughness.

Layup

Predicted values for fracture toughness of T300/5208 $[0^\circ_i/\pm45^\circ_j/90^\circ_k]_{ns}$ and $[0^\circ_i/\pm\alpha_j]_{ns}$ laminates are plotted in figures 6 and 7 against the percentage of 0° plies. These two families of laminates represent most layups of interest. The average values for fracture toughness of the three thickest laminates of

each layup in figure 2 and a $[0^\circ/\pm60^\circ]_{16s}$ T300/5208 laminate from [11] are shown for comparison. For both families of laminates, fracture toughness increases with the percentage of 0° plies, and the $[0^\circ_i/90^\circ_k]_{ns}$ subset has the lowest values for fracture toughness. For the $[0^\circ_i/\pm45^\circ_j/90^\circ_k]_{ns}$ family of laminates in figure 6, the $[0^\circ_i/\pm45^\circ_j]_{ns}$ subset, which are represented by the dash-dot curve, has the largest values for fracture toughness; and, for the $[0^\circ_i/\pm\alpha_j]_{ns}$ family of laminates in figure 7, the $[0^\circ_i/\pm17^\circ_j]_{ns}$ subset has the largest values for fracture toughness, but only slightly greater than that for a unidirectional laminate. For $\alpha < 17^\circ$, the fracture toughness increases with decreasing α.

Equation (5) is plotted in figures 6 and 7 as the horizontal dashed line. It predicts the same value for K_Q for all laminates with $E_y = E_x$, not just quasi-isotropic laminates. Many familiar layups have $E_y = E_x$, for example, $[0^\circ/90^\circ]_{ns}$, $[0^\circ/\pm45^\circ/90^\circ]_{ns}$, $[0^\circ/\pm60^\circ]_{ns}$, and $[\pm45^\circ]_{ns}$. These laminates have such different ultimate tensile strengths that one would not have expected the same fracture toughness. Notice that $[0^\circ_i/\pm\alpha_j]_{ns}$ laminates with $\alpha < 45^\circ$ in figure 7 can not have $E_y = E_x$.

The predictions in figures 6 and 7 were made assuming that the 0° plies are the principal load-carrying plies. Actually, for some very small percentage of 0° plies, the $\pm45^\circ$ and $\pm\alpha$ plies are the principal load-carrying plies. Thus, the curves are generally not valid very near the ordinate. (Fracture toughness can be predicted with equation (3) in these cases using $\alpha^* = 45^\circ$ or α.) On the other hand, for a large percentage of 0° plies, the curves may not be valid because of large matrix damage at the ends of the cuts.

The results of fracture tests were reported in [11] for several different T300/5208 quasi-isotropic laminates: $[0^\circ/\pm45^\circ/90^\circ]_{ns}$, $[90^\circ/\pm30^\circ]_{ns}$, and $[0^\circ/\pm60^\circ]_{ns}$. The test values for fracture toughness for the thickest are plotted in figure 8 along with the predicted value of 1.11 GPa$\sqrt{\text{mm}}$. The values agree fairly well. (The values in [11] were not calculated for the maximum loads. The values in figure 8 were calculated with equation (4) for maximum loads obtained by private communications with the authors.)

Values of K_Q/F_{tu} for the T300/5208 $[0^\circ_i/\pm45^\circ_j/90^\circ_k]_{ns}$ and $[0^\circ_i/\pm\alpha_j]_{ns}$ laminates, are plotted in figures 9 and 10. For both families of laminates, the $[0^\circ_i/\pm45^\circ_j]_{ns}$ subset has the highest values (least notch sensitive) and the

$[0^\circ_i/90^\circ_k]_{ns}$ subset has the lowest values (most notch sensitive). Although the $[0^\circ_i/\pm 17^\circ_j]_{ns}$ subset has the highest values for K_Q, it does not does not have the highest values for K_Q/F_{tu}.

In figure 9, the curves for K_Q/F_{tu} for a given percentage of 45° plies are relatively flat. Thus, replacing 0° by 90° plies, or vice versa, has little effect on notch sensitivity, whereas replacing 45° plies by 0° or 90° plies increases notch sensitivity significantly, and vice versa. Notice that the curves for a given percentage of 45° plies are slightly concave upward and have a minimum for laminates with $E_y = E_x$. The range of K_Q/F_{tu} values for metals is also shown in figure 9 for comparison. The metals are generally less notch sensitive than composites.

Because the notch sensitivity of $[0^\circ_i/\pm\alpha_j]_{ns}$ laminates in figure 10 does not vary monotonically with the angle α, a small graph was inserted to show that K_Q/F_{tu} is approximately symmetric about $\alpha = 45^\circ$, where it is greatest. For $20^\circ < \alpha < 70^\circ$, notch sensitivity increases with the percent of 0° plies. However, for $\alpha < 20^\circ$ and $\alpha > 70^\circ$, K_Q is nearly a constant. A curve for $E_y = E_x$ was not plotted in figure 10 because it does not apply to laminates with $\alpha < 45^\circ$ and would be ambiguous.

SURFACE CUTS

Except for shallow surface cuts, thick resin-matrix composites fail in two stages: first, the cut ligament or sublaminate, which also delaminates at the bottom of the cut, and then, with additional load, the uncut ligament. See figure 11. The two stages of failure are referred to as first- and remaining-ligament failure. The delamination can initiate prior to failure of the first ligament, but it does not spread throughout the specimen until the first ligament fails. For shallow surface cuts, the laminate fails in one stage as a metal. The stress for first-ligament failure decreased with increasing surface cut size according to linear elastic fracture mechanics, and the stress for remaining-ligament failure varied inversely with its thickness, t - a, much as an uncut laminate. For thick graphite/epoxy laminates, impacted specimens failed similarly, indicating that impact damage and surface cuts are equivalent [1,2].

The failure of the first ligament was assumed to occur when the maximum stress intensity factor along the front of the crack-like cut was equal to the fracture toughness K_Q. Using the stress intensity factor equation in the

Appendix for a semi-elliptical surface crack in an isotropic homogeneous plate, the stress for first-ligament failure S_c is given by

$$S_c = \frac{K_Q}{\left[\frac{\pi a F(a/t, a/c, c/W, \phi)}{Q}\right]^{1/2}} \tag{10}$$

The value of the elliptical angle ϕ in equation (10) that corresponds to the maximum value of stress intensity factor was used to make the predictions. Equation (10) should be valid for composite laminates that are quasi-isotropic or nearly quasi-isotropic and for cuts that are large compared to the thickness of ply groups and matrix damage.

Test values from [12] and predicted values for stresses for first- and remaining-ligament failure are plotted in figure 12 for $[0^\circ/\pm45^\circ/90^\circ]_{10s}$ T300/5208 specimens with semi-elliptical surface cuts of various sizes. The predicted value of 1.11 GPa$\sqrt{\text{mm}}$ was used for K_Q. Because the laminate has 20 ply groups, it is thick enough for equation (3) to be valid. The dashed curve for remaining-ligament strength was calculated with

$$S_r = (1 - \frac{a}{t})E_y \epsilon_{tuf} \tag{11}$$

The test values for first-ligament strength in figure 12 are averages of five values, and those for remaining-ligament strength are averages of two to four values. (The remaining-ligament strengths were obtained by private communications with the authors [12].) The stresses were calculated using the gross area tW. The specimens with $c/a = 0.5$ and 1.0 were 25.4 mm wide, and those with $c/a = 3.9$ were 50.8 mm wide. Except for the smallest values of cut depth, the test and predicted strengths agree. For the smallest values of cut depth, the laminates failed as one part, much like metals, and the first-ligament strengths are overpredicted. The tests were conducted in a stroke-control mode allowing the load to drop when the first ligament failed. Thus, the failures of the first ligaments of specimens with $c/a = 1.0$ were arrested. Subsequent loading revealed that the remaining-ligament strengths were lower than the first-ligament strengths, as predicted by the solid and dashed curves. For $c/a = 3.9$, the remaining-ligament strengths were higher than the first-ligament strengths. But, for $c/a = 0.5$, the first failures were not arrested, and the composite specimens behaved more like metal specimens.

Similar results are plotted in figures 13(a) and 13(b) for a 36-mm-thick AS4/HBRF-55A laminate that was filament-wound. The data were reported in [1] and [13]. The specimens were cut from a 0.76-meter-diameter cylinder. The laminate consisted of approximately 19 layers with 0° orientation and 32 layers with $\pm56.5^\circ$ orientation (relative to the axis of the cylinder and the loading direction of the specimens). The thickness of each filament-wound layer is three times that of each tape layer of the T300/5208 laminates. The filament-wound laminate is unsymmetric. However, the grips fixed the specimen ends and prevented bending so that the laminate behaved as though it were symmetric. Thus, the elastic constants were calculated assuming that the laminate is

symmetric. The results were E_x = 30.6 GPa, E_y = 39.0 GPa, G_{xy} = 19.7 GPa, ν_{xy} = 0.351, and ν_{yx} = 0.447. Thus, the laminate is not very different from a quasi-isotropic laminate. The curves for first-ligament strength in figure 13(a) were predicted with equation (10) and a value of K_Q = 0.949 GPa$\sqrt{\text{mm}}$. from equation (3). The curve for remaining-ligament strength in figure 13(b) was calculated with

$$S_r = E_y \epsilon_{tuf} \tag{12}$$

where E_y was calculated for the uncut sublaminate assuming a thickness of t - a. The large and small drops in stress correspond to removing the stiff 0° layers and the more flexible $\pm 56.5^\circ$ layers, respectively. The curve is convex in the overall sense because most of the 0° layers are closer to the bottom of the laminate. Except for very small values of cut depth, the test and predicted first-ligament strengths agree. For cut depths less than about 5 mm, the laminates failed as one part. The remaining-ligament strengths are overpredicted a little for the intermediate values for cut depth.

When the applied load is fixed (not allowed to drop at first failure), laminates can only fail in two stages if the thickness is large enough that the first-ligament strength is less than the remaining-ligament strength like that in figure 11. The minimum thickness occurs when the two curves for load versus a/t in figure 11 are tangent. The conditions for the curves being tangent are $S_c = S_r$ and $\frac{\partial S_c}{\partial (a/t)} = \frac{\partial S_r}{\partial (a/t)}$, where S_c and S_r are given by equations (10) and (11). For small a/t and c/W, the point of tangency occurs at a/t = 1/3 and

$$t_{min} = \frac{Q(4.5K_Q)^2}{3\pi(F_{tu}M_1 g)^2} \tag{13}$$

Values for t_{min} were calculated with equation (13) for $[0^\circ_i/\pm 45^\circ_j/90^\circ_k]_{ns}$ T300/5208 laminates and plotted in figure 14. The right-hand side of equation (13) increases with increasing a/c. A value of a/c = 0 and $\phi = 0^\circ$ was assumed in order to get the smallest values for t_{min}. Because t_{min} in equation (13) is proportional to $(K_Q/F_{tu})^2$, the curves in figure 14 resemble those for K_Q/F_{tu} in figure 9. The smallest values for t_{min} correspond to the most notch sensitive laminates and vice versa.

Values for t_{min} for a/c = 1 are 2.9 times larger than those in figure 14 for a/c = 0. Thus, flaw shape has a significant effect on t_{min}. As a/c

increases and the surface cut becomes more like a through-the-thickness cut, t_{min} increases, eliminating two-part failure.

CONCLUSIONS

A parametric study was made of $[0^\circ_i/\pm45^\circ_j/90^\circ_k]_{ns}$ and $[0^\circ_i/\pm\alpha_j]_{ns}$ laminates to determine how fiber and matrix properties as well as layup affect the fracture toughness K_Q and notch insensitivity K_Q/F_{tu}. The values for K_Q were predicted from lamina properties using the general fracture toughness parameter Q_c. Experimental values of K_Q for through-the-thickness cuts and strengths for surface cuts were compared to the predictions. The following conclusions were reached:

1. Fiber properties are very important.
   a. K_Q increases directly in proportion to fiber strength, fiber volume fraction, and $[1 + E_{22}/E_{11} + \ldots]$, where E_{11} and E_{22} are Young's modulae of the laminae and 1 is parallel to the fiber direction.
   b. In hybrids, K_Q is larger when the off-direction plies are stiffer than those in the loading direction (0° plies).
2. Matrix properties are not important as long as the fibers carry most of the load and the matrix is strong enough not to crack or delaminate extensively.
3. Layup is very important.
   a. K_Q is largest for $[0^\circ_i/\pm17^\circ_j]_{ns}$ laminates and smallest for $[0^\circ_i/90^\circ_k]_{ns}$ laminates.
   b. K_Q is the same for all laminates with equal longitudinal and transverse Young's modulae, like $[\pm45^\circ]_{ns}$, $[0^\circ/\pm45^\circ/90^\circ]_{ns}$, $[0^\circ/90^\circ]_{ns}$, etc.
   c. $[0^\circ_i/\pm45^\circ_j]_{ns}$ laminates are the least notch sensitive (largest value for K_Q/F_{tu}), and $[0^\circ_i/90^\circ_k]_{ns}$ laminates are the most notch sensitive.
4. Unlike most metals, fiber properties and layup can be selected to increase K_Q and F_{tu} without increasing notch sensitivity (decreasing K_Q/F_{tu}).

5. Unlike metals, thick graphite/epoxy laminates with surface cuts can fail in two stages, giving some redundancy. First, the cut laminae failed, and then the uncut laminae. When the cut laminae failed, they delaminated from the uncut laminae.

   a. Surface flaw analysis can be used directly to predict the stresses for the first failure when the cut depth is large compared to ply thickness.
   b. The final strength is equal to that of an uncut laminate of reduced thickness.
   c. Laminates with shallow cuts failed in one stage, much like metals.

APPENDIX

For an isotropic, homogeneous material, the stress intensity factor along the front of a semi-elliptical surface crack is given [14] by

$$K = S\left[\frac{(\pi a)F(a/t, a/c, c/W, \phi)}{Q}\right] \tag{14}$$

where ϕ specifies the location along the crack front in terms of the parametric angle of the ellipse,

$$F = [M_1 + M_2(\tfrac{a}{t})^2 + M_3(\tfrac{a}{t})^4]gf_\phi f_w$$

and

$$f_w = \{\sec[(\tfrac{\pi c}{W})(\tfrac{a}{t})^{1/2}]\}^{1/2}$$

For $a/c \leq 1$,

$$Q = 1 + 1.464(\tfrac{a}{c})^{1.65}$$

$$M_1 = 1.13 - 0.09(\tfrac{a}{c})$$

$$M_2 = -0.54 + \frac{0.89}{0.2 + \frac{a}{c}}$$

$$M_3 = 0.5 - \frac{1}{0.65 + \frac{a}{c}} + 14(1 - \tfrac{a}{c})^{24}$$

$$g = 1 + [0.1 + 0.34(\tfrac{a}{t})^2][1 - \sin\phi]^2$$

$$f_\phi = [(\tfrac{a}{c})^2\cos^2\phi + \sin^2\phi]^{1/4}$$

and for $a/c > 1$,

$$Q = 1 + 1.464\left(\frac{c}{a}\right)^{1.65}$$

$$M_1 = \left[1 + 0.04\left(\frac{c}{a}\right)\right]\left(\frac{c}{a}\right)^{1/2}$$

$$M_2 = 0.2\left(\frac{c}{a}\right)^{-4}$$

$$M_3 = -0.11\left(\frac{c}{a}\right)^{4}$$

$$g = 1 + \left[0.1 + 0.35\left(\frac{c}{a}\right)\left(\frac{a}{t}\right)^2\right][1 - \sin\phi]^2$$

$$f_\phi = \left[\left(\frac{c}{a}\right)^2 \sin^2\phi + \cos^2\phi\right]^{1/4}$$

Equation (14) was derived using results from a finite element analysis.

REFERENCES

1. Poe, Jr., C. C.; Illg, W.; and Garber, D. P.: A Program to Determine the Effect of Low-Velocity Impacts on the Strength of the Filament-Wound Rocket Motor Case for the Space Shuttle. NASA TM-87588, September 1985.

2. Poe, Jr., C. C.; Illg, W.; and Garber, D. P.: Tension Strength of a Thick Graphite/Epoxy Laminate after Impact by a 1/2-In.-Radius Impacter. NASA TM-87771, July 1986.

3. Poe, Jr., C. C.: Fracture Toughness of Boron/Aluminum Laminates with Various Proportions of 0° and $\pm 45^\circ$ Plies. NASA TP-1707, 1980.

4. Poe, Jr., C. C.: A Unifying Strain Criterion for Fracture of Fibrous Composite Laminates. Engineering Fracture Mechanics, vol. 17, no. 2, 1983, pp. 153-171.

5. Dharani, L. R.; Jones, W. F.; and Goree, James G.: Mathematical Modeling of Damage in Uni-Directional Composites. Engineering Fracture Mechanics, vol. 17, no. 6, 1983, pp.555-573.

6. Harris, C. E.; and Morris, D. H.: Fracture Behavior of Thick, Laminated Graphite/Epoxy Composites. NASA CR-3784, 1984.

7. Harris, C. E.; and Morris, D. H.: A Comparison of the Fracture Behavior of Thick Laminated Composites Utilizing Compact Tension, Three-Point Bend, and Center-Cracked Tension Specimens. Fracture Mechanics: Seventeenth Volume, ASTM STP 905, American Society for Testing and Materials, 1986, pp. 124-135.

8. Whitcomb, John D.; and Raju, Ivatury S.: Analysis of Interlaminar Stresses in Thick Composite Laminates With and Without Edge Delamination. Delamination and Debonding of Materials, ASTM STP 876, American Society for Testing and Materials, 1985, pp. 69-94.

9. Kennedy, John M.: Fracture Behavior of Hybrid Composite Laminates. A Collection of Technical Papers, Part 1: Structures and Materials, AIAA/ASME/ASCE/AHS 24th Structures, Structural Dynamics and Materials Conference, May 1983, pp. 68-73. (Available as AIAA-83-0804.)

10. Poe, Jr., C. C.: Fracture Toughness of Fibrous Composite Materials. NASA TP-2370, November 1984.

11. Harris, C. E.; and Morris, D. H.: A Damage Tolerant Design Parameter for Graphite/Epoxy Laminated Composites. Journal of Composites Technology and Research, vol. 7, no. 3, Fall 1985, pp. 77-81.

12. Harris, C. E.; and Morris, D. H.: Fracture of Thick Graphite/Epoxy Laminates with Part-Through Surface Flaws. Composite Materials: Fatigue and Fracture, ASTM STP 907, American Society for Testing and Materials, 1986, pp. 100-114.

13. Harris, C. E.; and Morris, D. H.: Preliminary Report on Tests of Tensile Specimens with a Part-Through Surface Notch for a Filament Wound Graphite/Epoxy Material. NASA CR-172545, March 1985.

14. Newman, Jr., J. C.; and Raju, I. S.: Stress-Intensity Factor Equations for Cracks in Three-Dimensional Finite Bodies. Fracture Mechanics: Fourteenth Symposium--Volume I: Theory and Analysis, ASTM STP 791, American Society for Testing and Materials, 1983, pp. I-238-I-268.

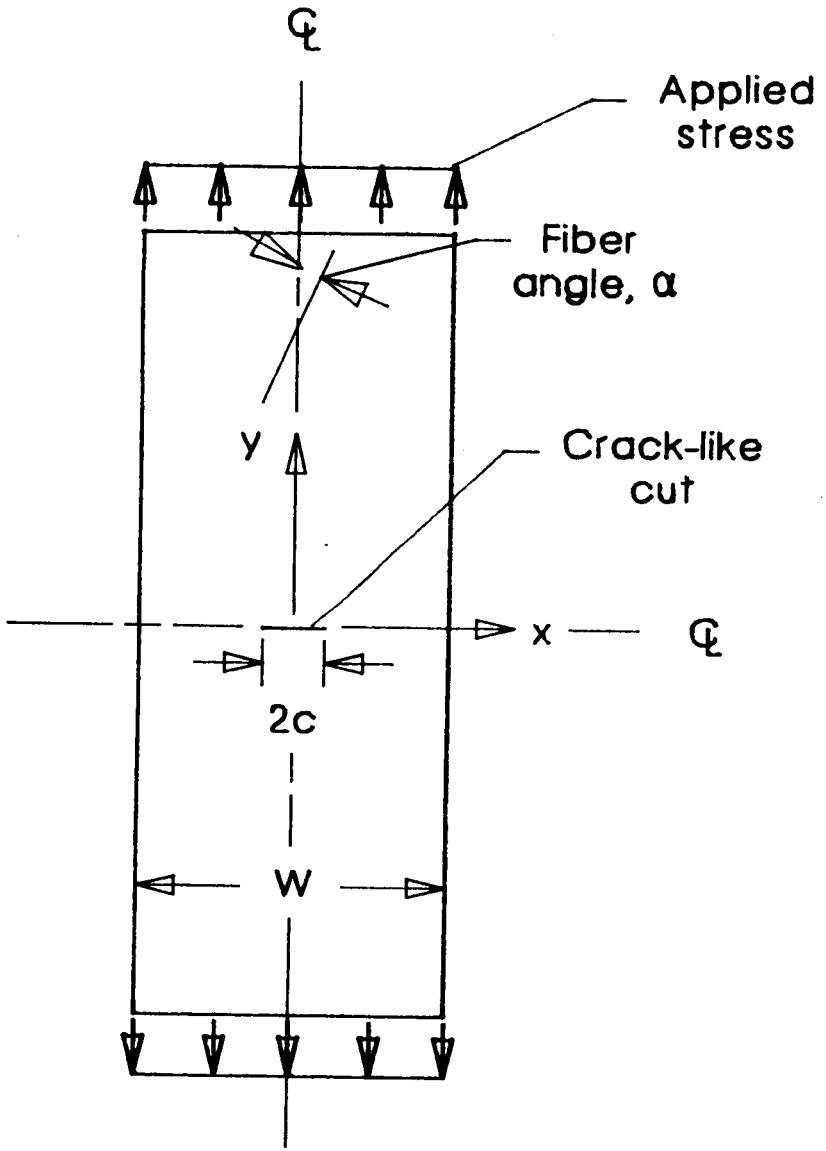

Figure 1.- Coordinate system and specimen configuration.

FIG1.OMA

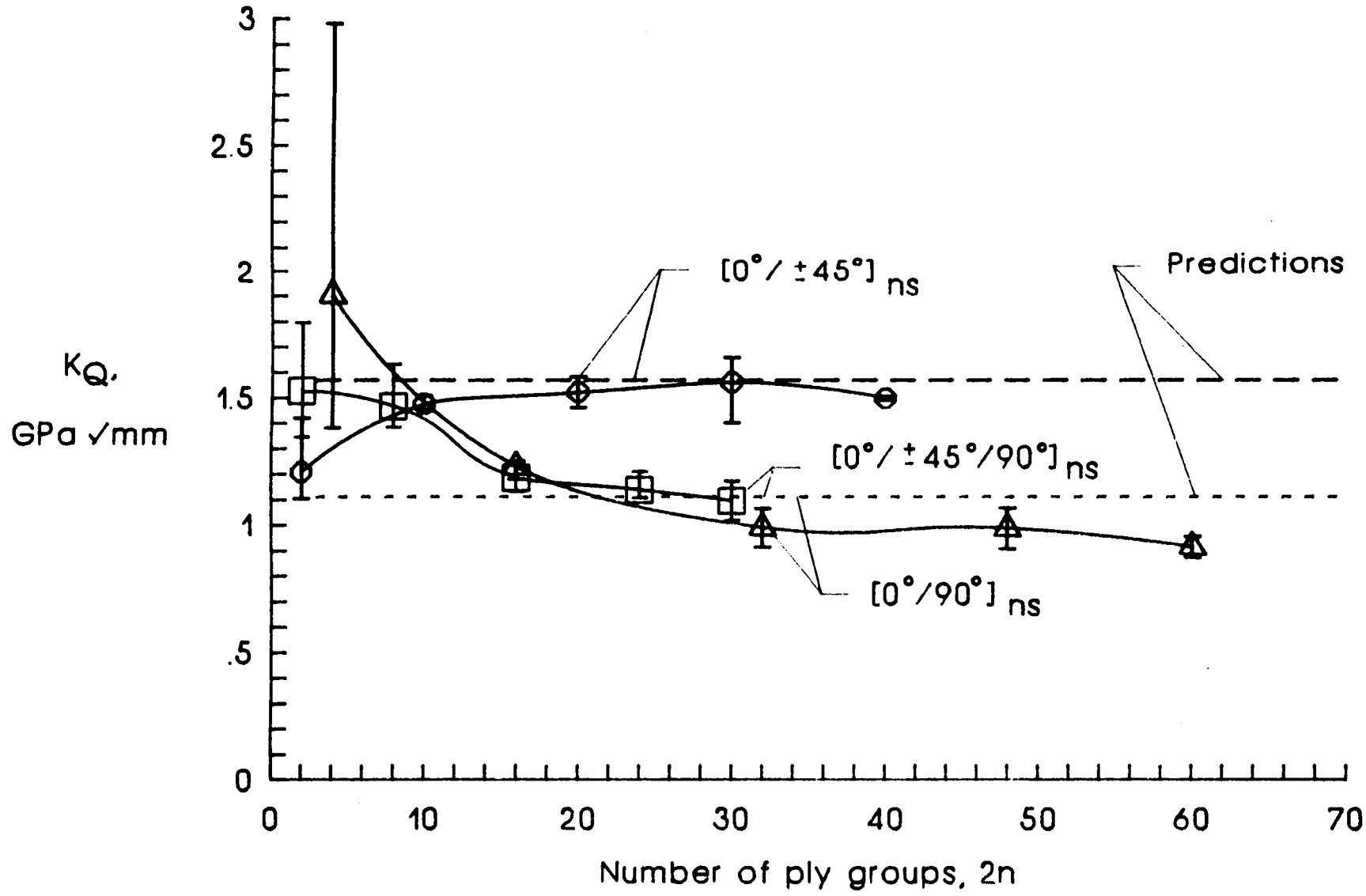

Figure 2.- Fracture toughness versus thickness for T300/5208 laminates.

FIG2.OMA

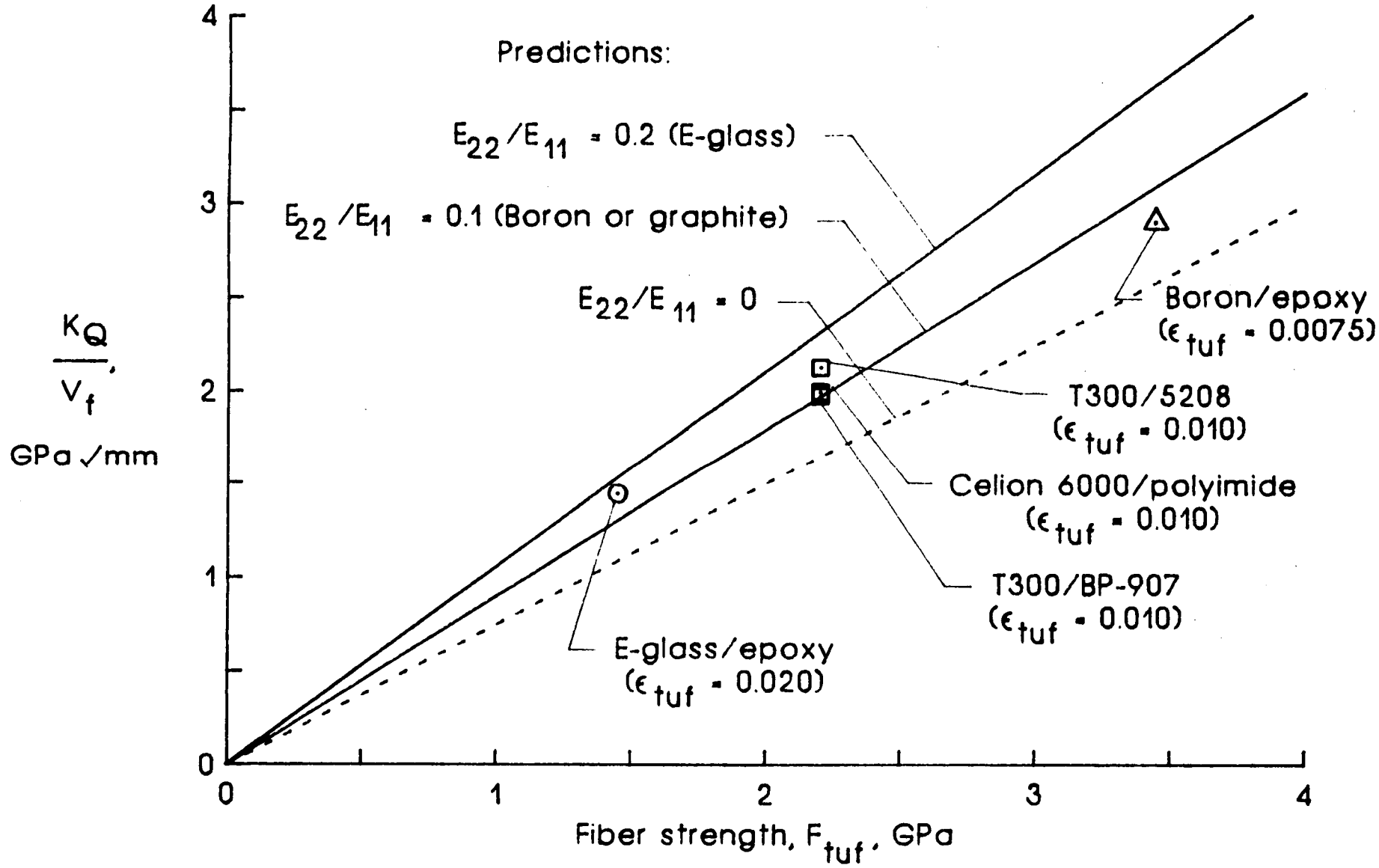

Figure 3.- Effect of fiber strength on fracture toughness of $[0°/\pm45°/90°]_s$ and $[0°/\pm45°/90°]_{2s}$ laminates.

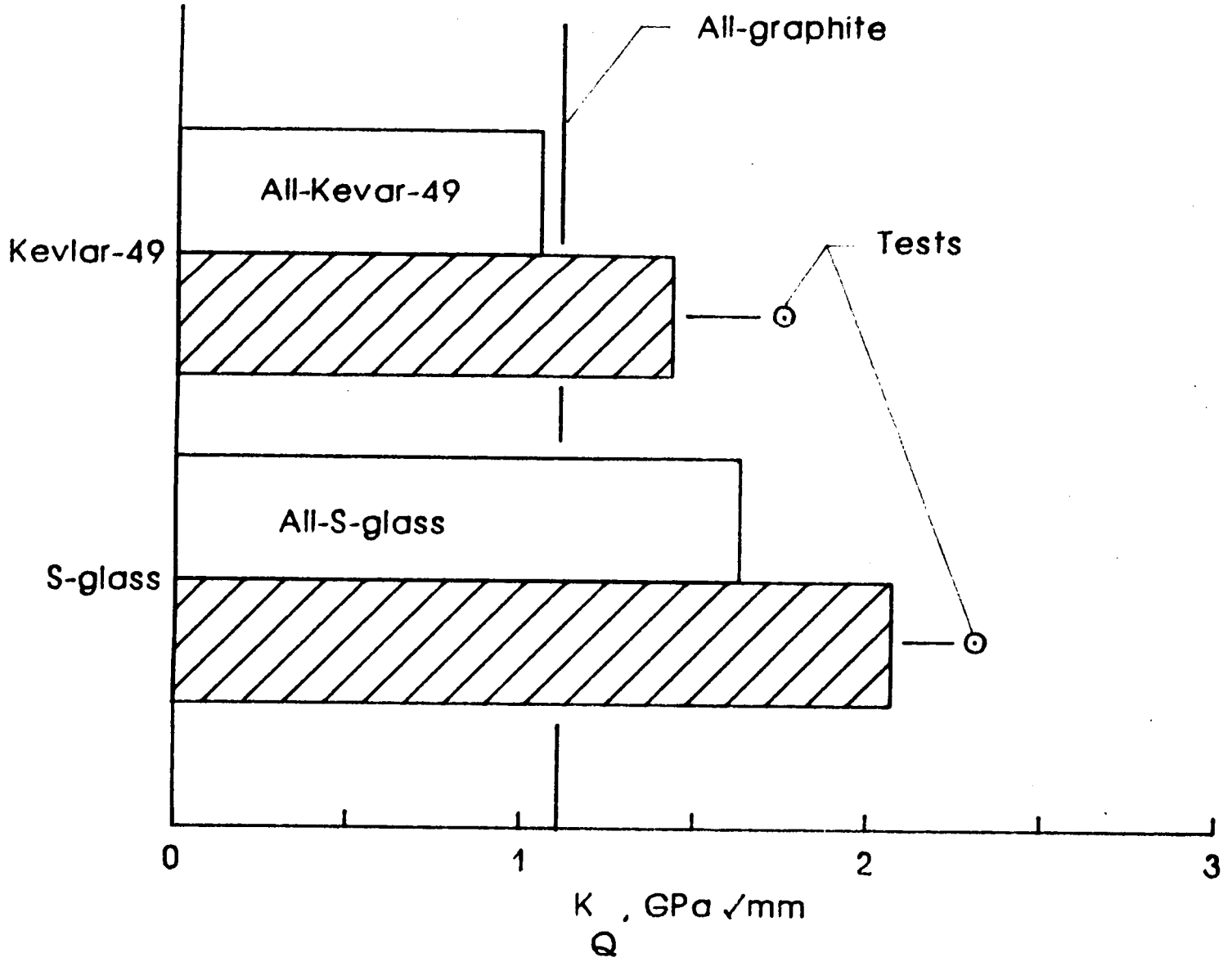

Figure 4.- Fracture toughness predictions for S-glass-graphite and Kevlar-49-graphite $[45^{\circ}/0^{\circ}/-45^{\circ}/90^{\circ}]_{s}$ hybrid laminates. For hybrids, 45° and 90° plies are T300 graphite. Resin is 5208 epoxy.

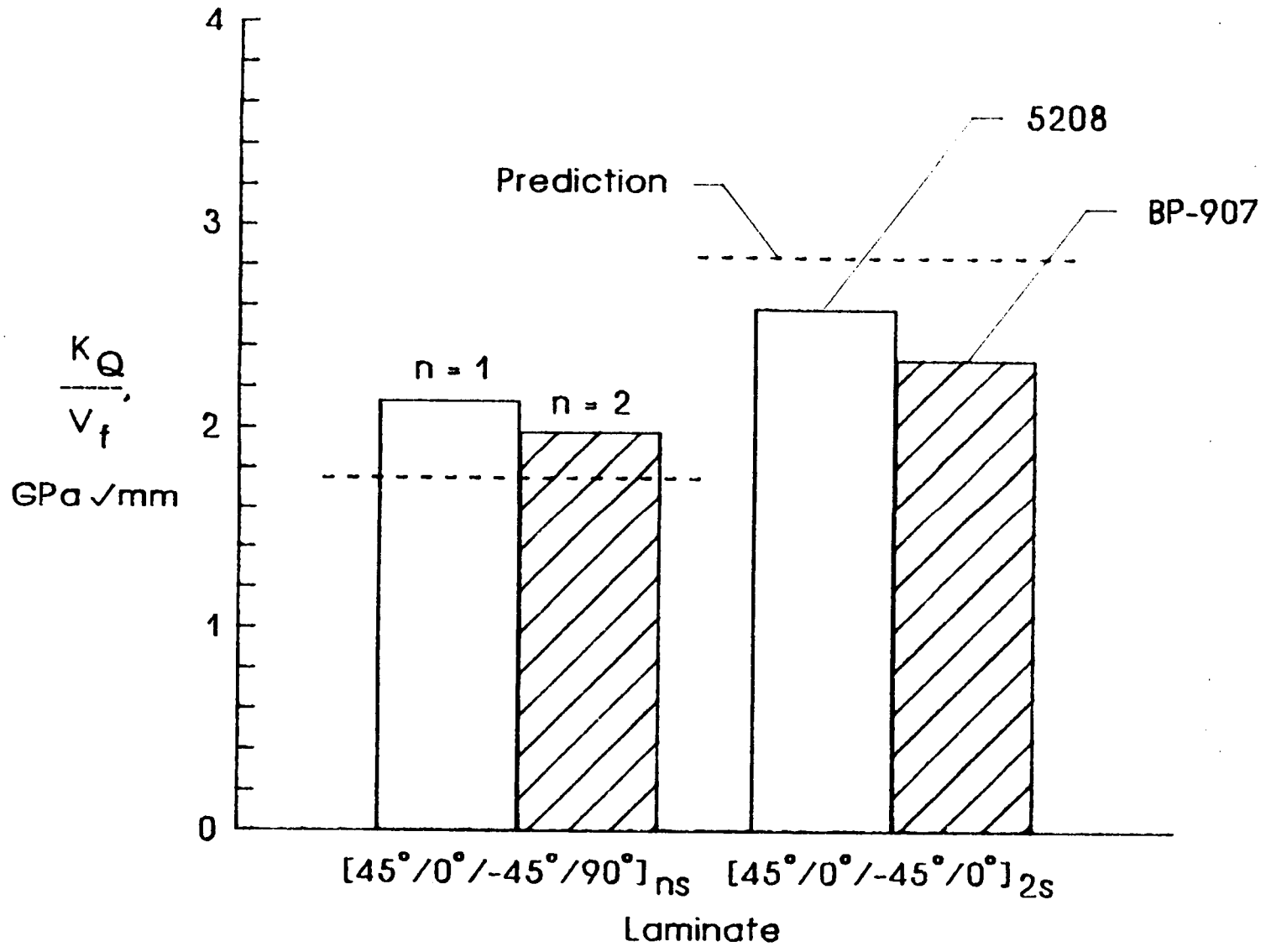

Figure 5.- Measured and predicted fracture toughness of T300/5208 and T300/BP-907 laminates.

FIG5.OMA

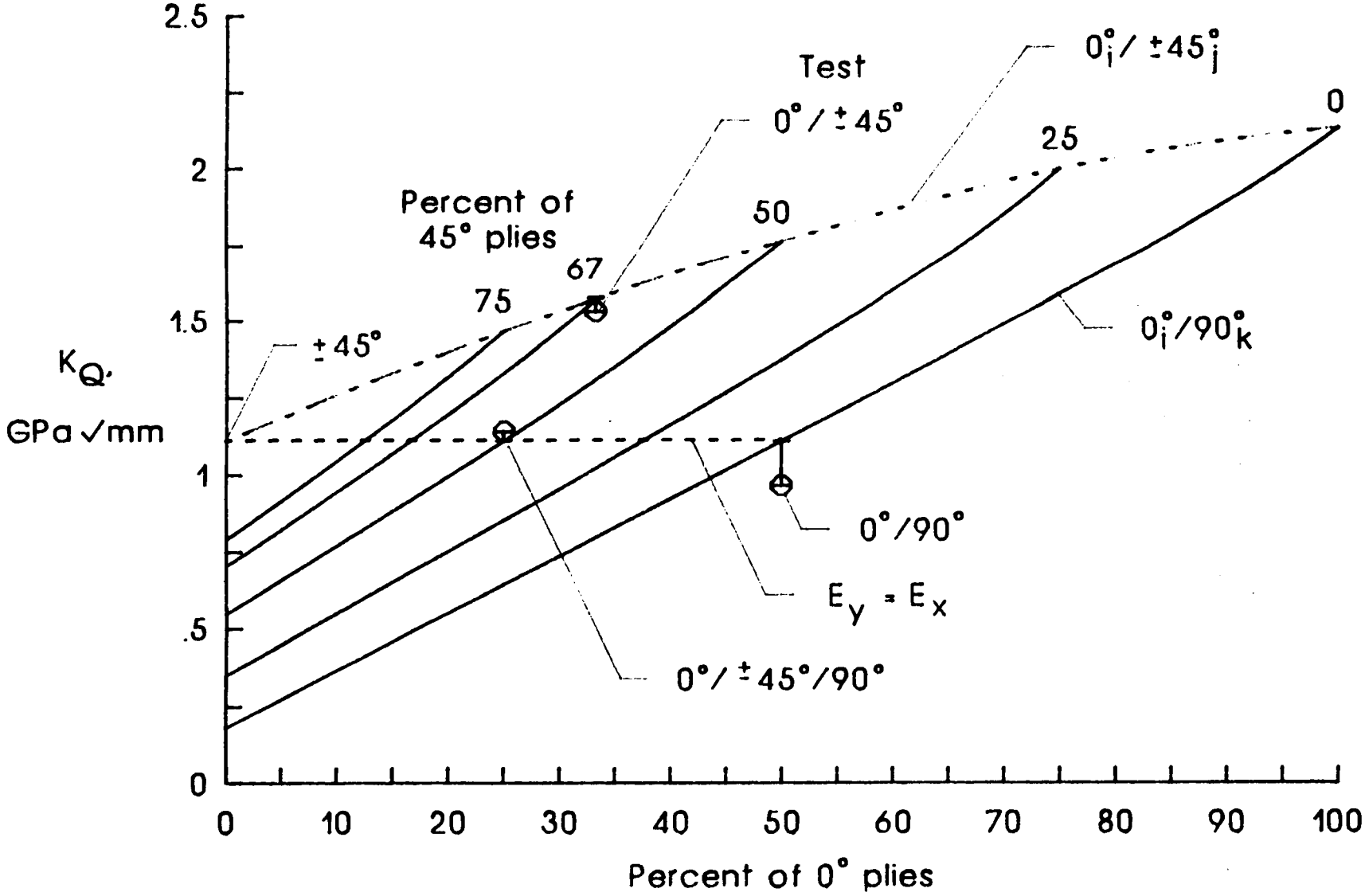

Figure 6.- Predicted fracture toughness of $[0^\circ_i / \pm 45^\circ_j / 90^\circ_k]_{ns}$ T300/5208 laminates.

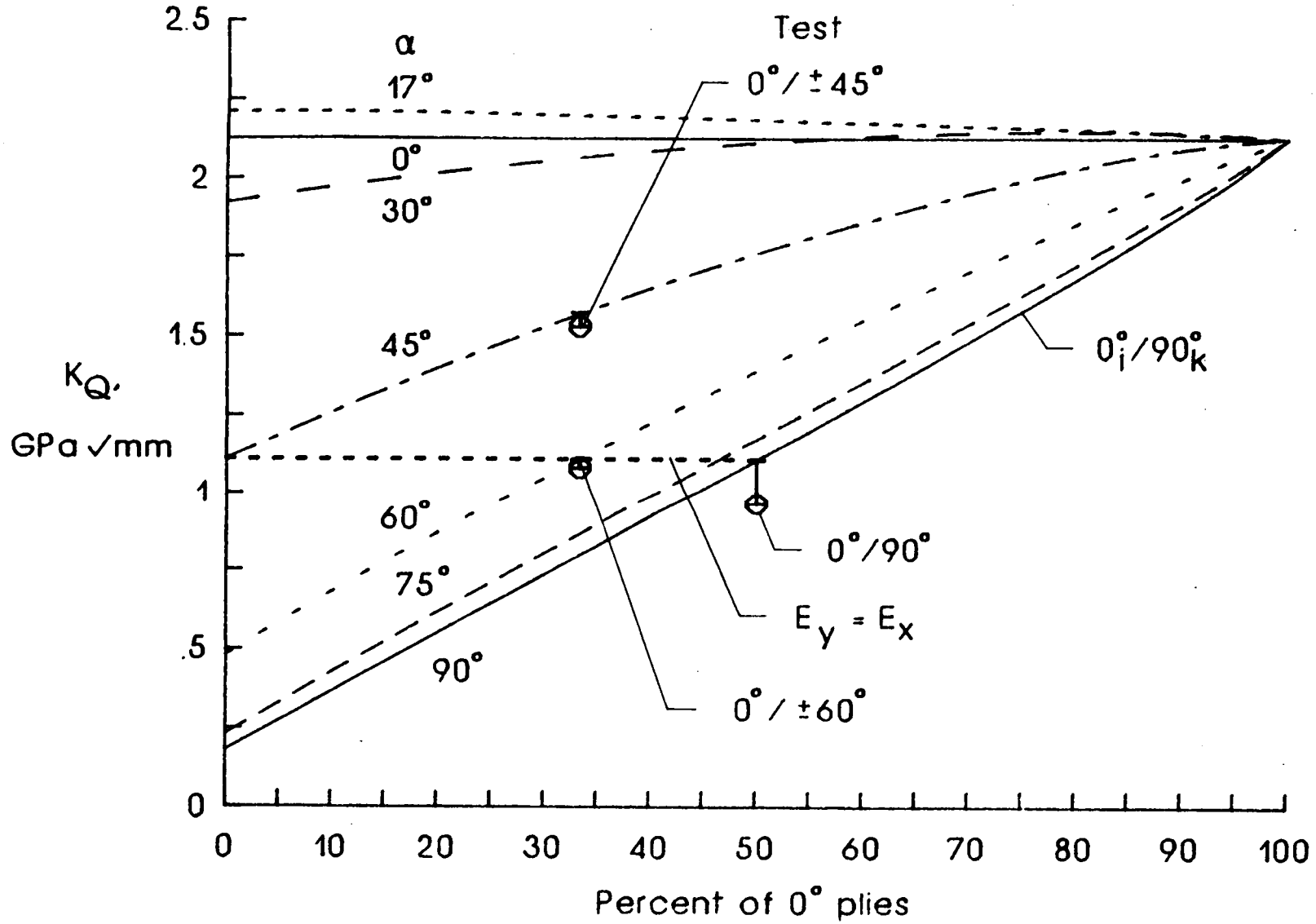

Figure 7.- Predicted fracture toughness $[0^\circ_i/\pm\alpha_j]_{ns}$ T300/5208 laminates.

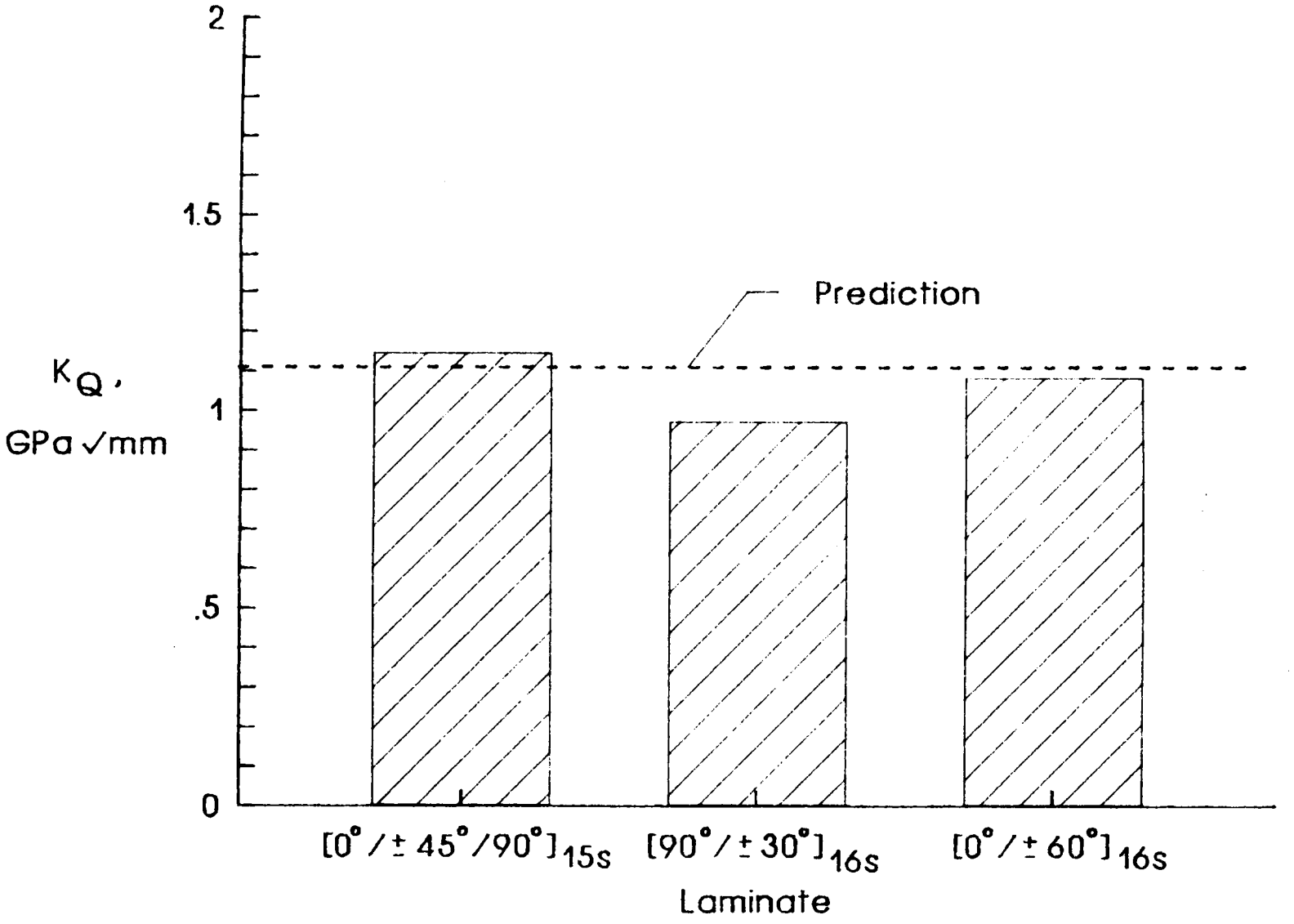

Figure 8.- Measured and predicted fracture toughness of T300/5208 quasi-isotropic laminates.

PLOT8.OMA

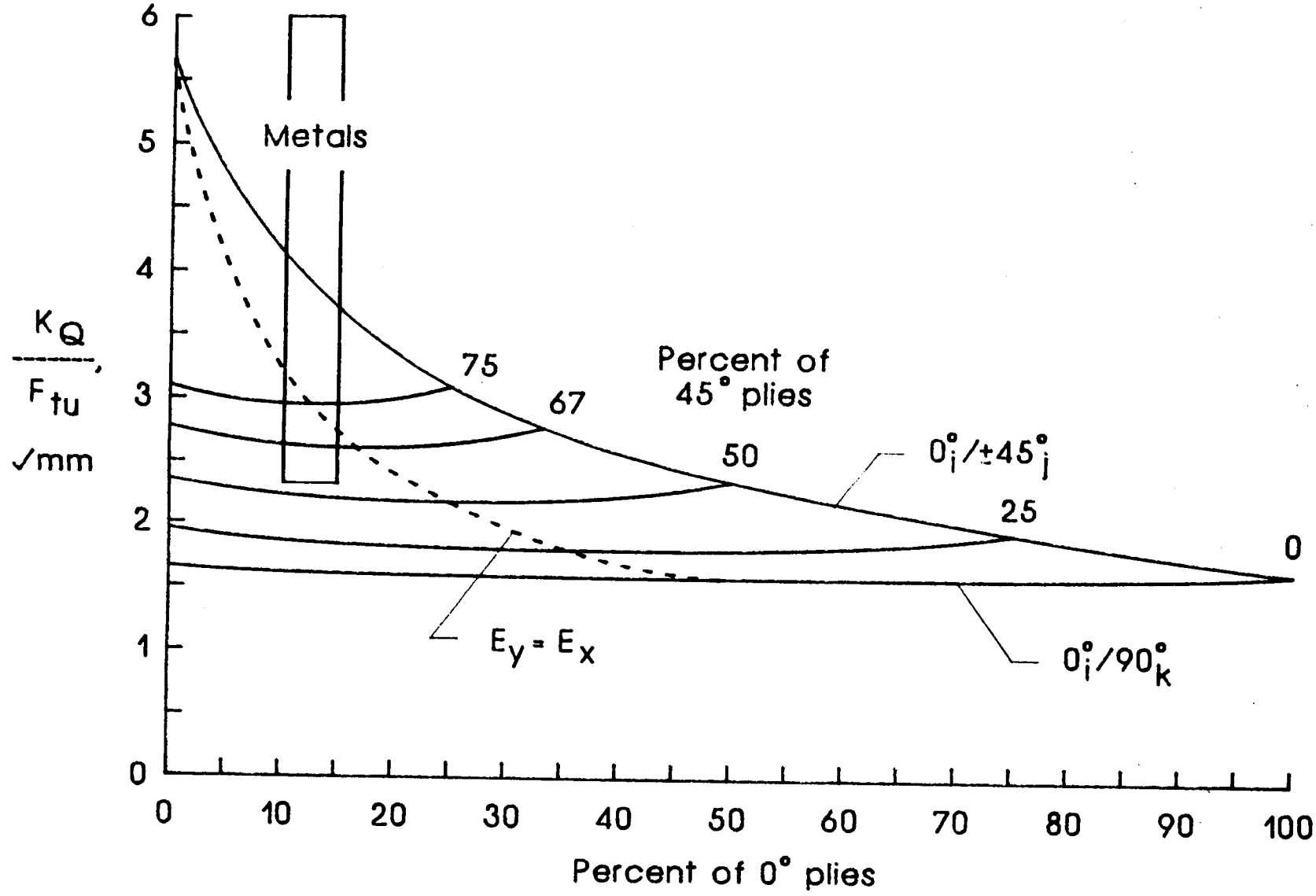

Figure 9.- Predicted notch sensitivity of $[0^\circ_i/\pm45^\circ_j/90^\circ_k]_{ns}$ T300/5208 laminates.

PLOT2F.OMA

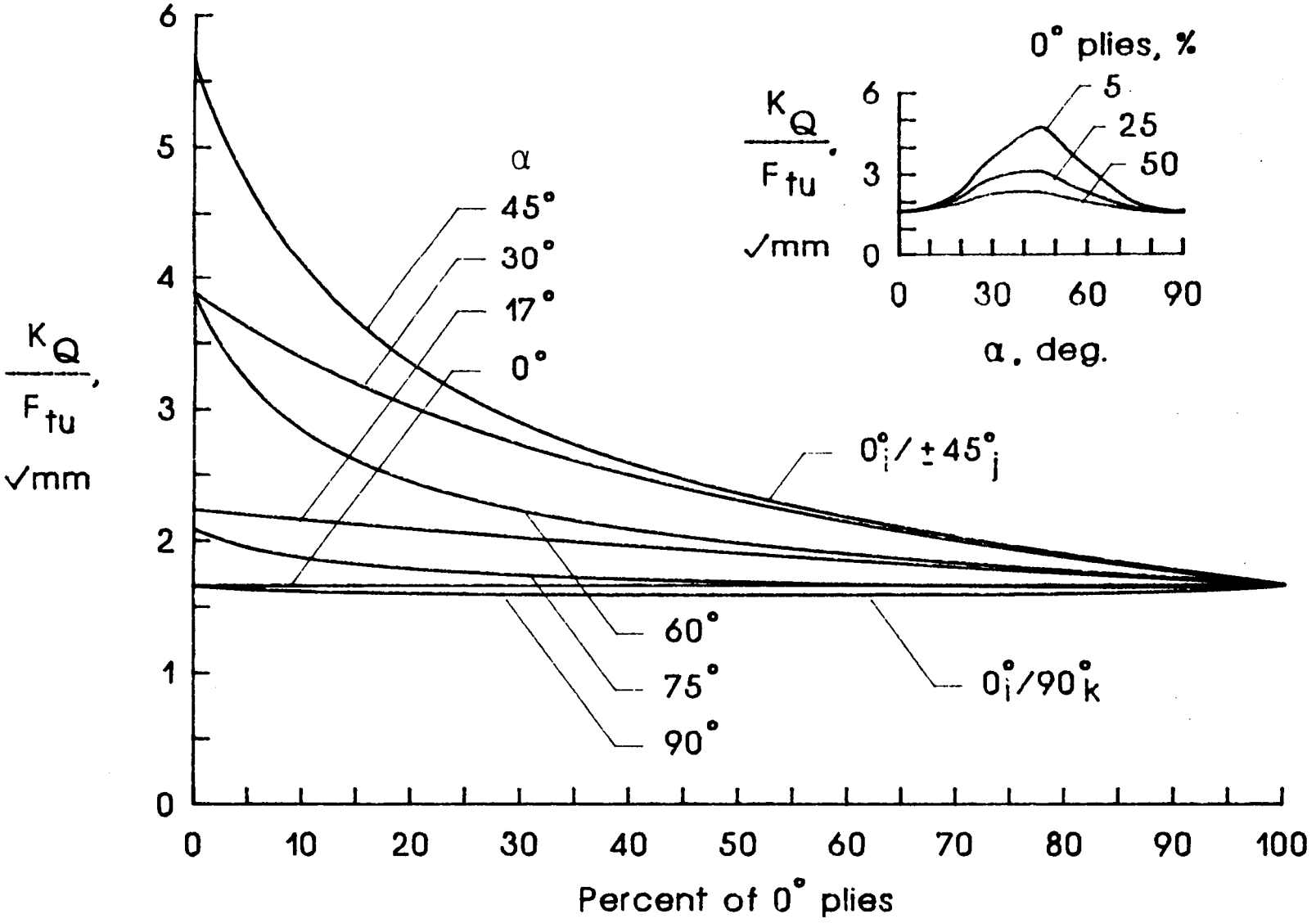

Figure 10.- Predicted notch sensitivity of $[0^\circ_i/\pm\alpha_j]_{ns}$ T300/5208 laminates.

PLOT1G.OMA

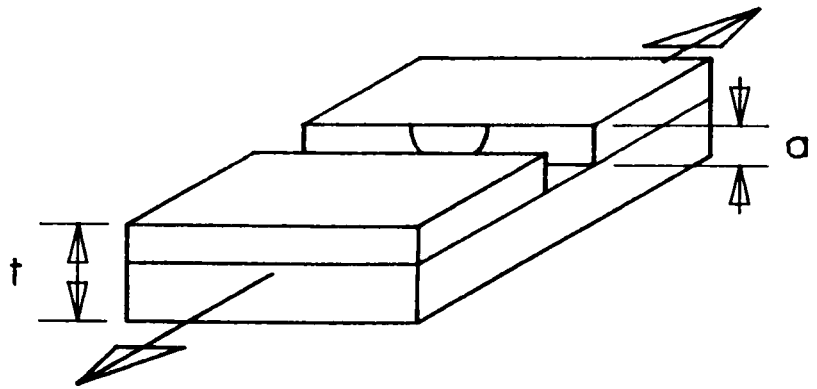

FIRST-LIGAMENT FAILURE

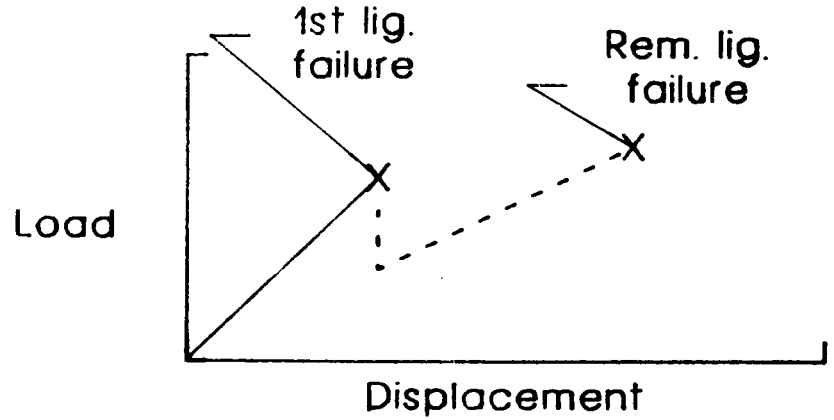

REGION A, TWO-PART FAILURE

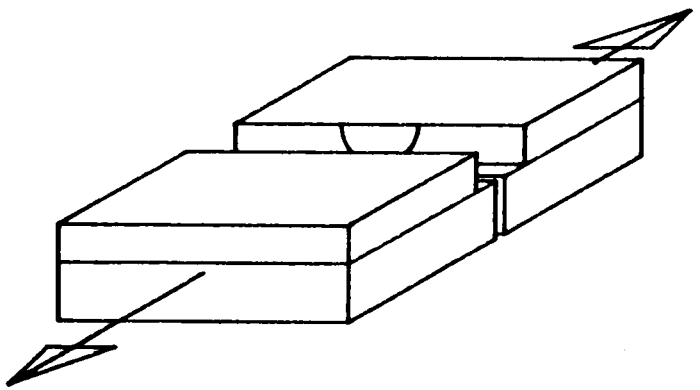

REMAINING-LIGAMENT FAILURE

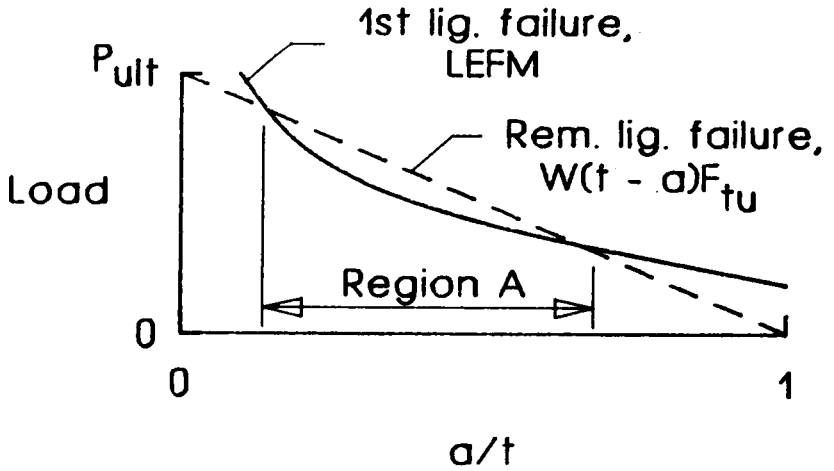

STRENGTH

Figure 11.- Two-part failure for thick composites with surface cuts.

FIG11.OMA

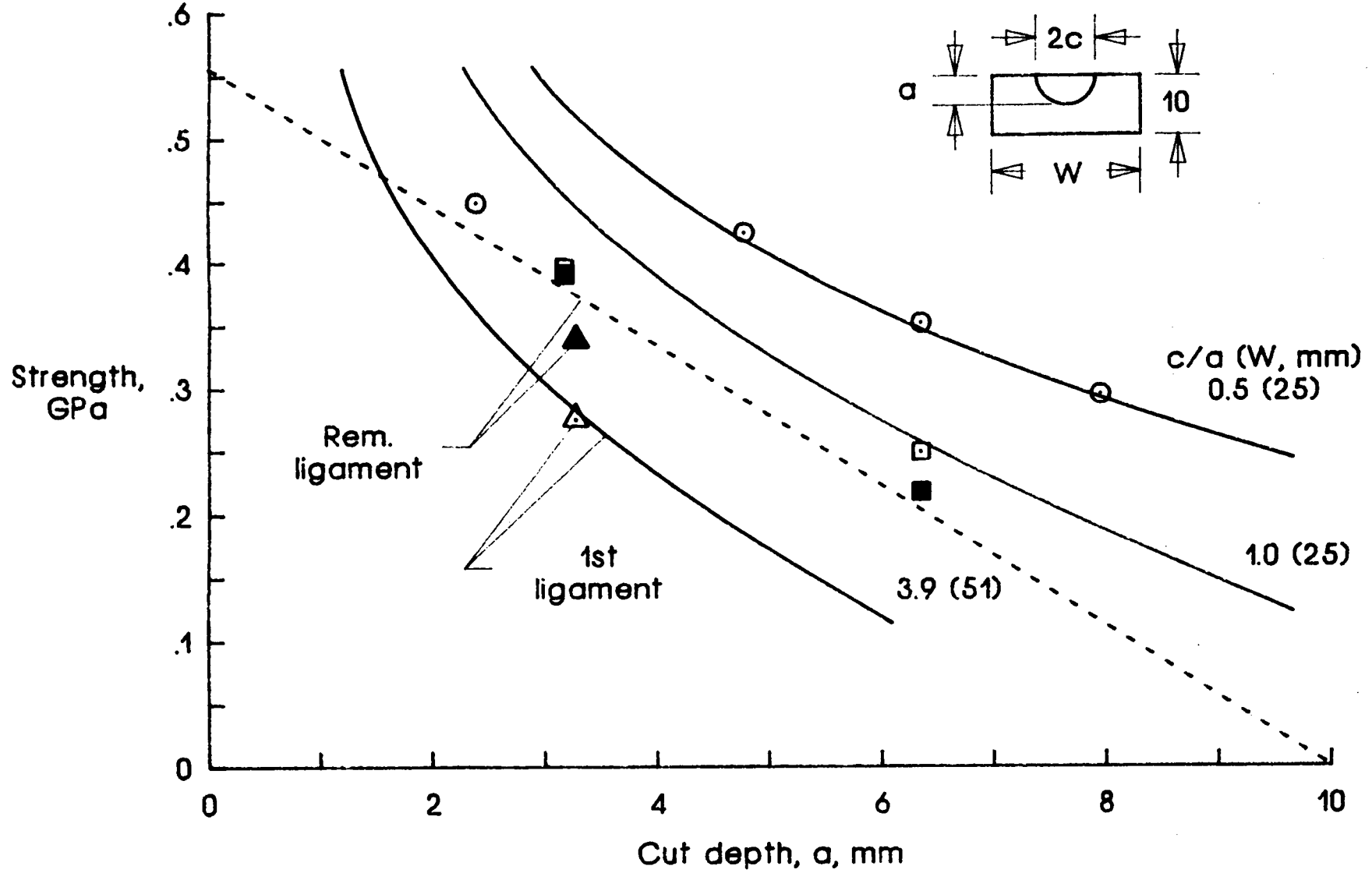

Figure 12.- Strength versus surface cut depth for a $[0°/\pm45°/90°]_{10s}$ T300/5208 laminate.

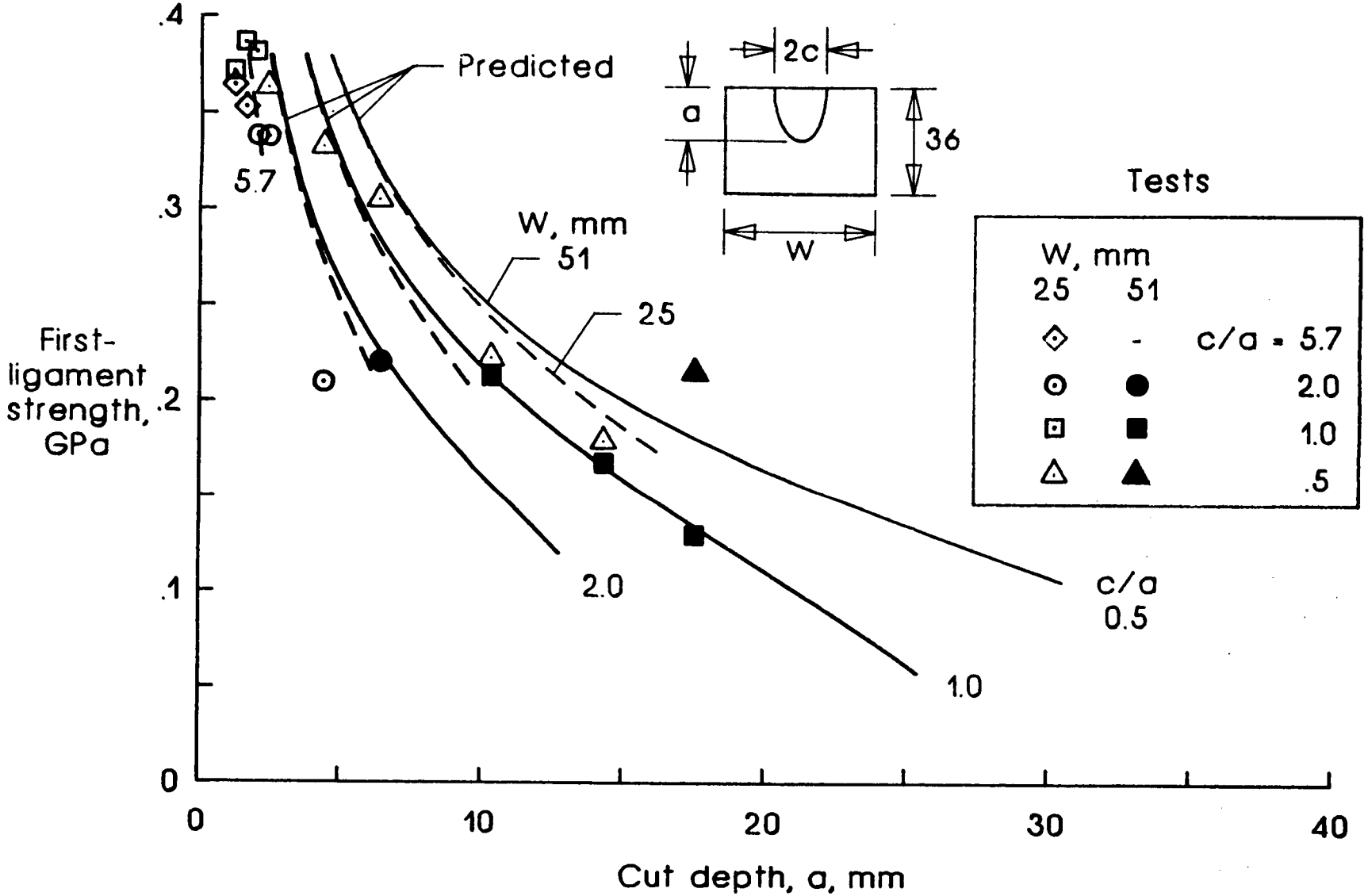

(a) First-ligament strength.

Figure 13.- Strength versus surface cut depth for a $[0^{\circ}_{19}/(+56.5^{\circ}/-56.5^{\circ})_{32}]$ AS4/HBRF-55A laminate.

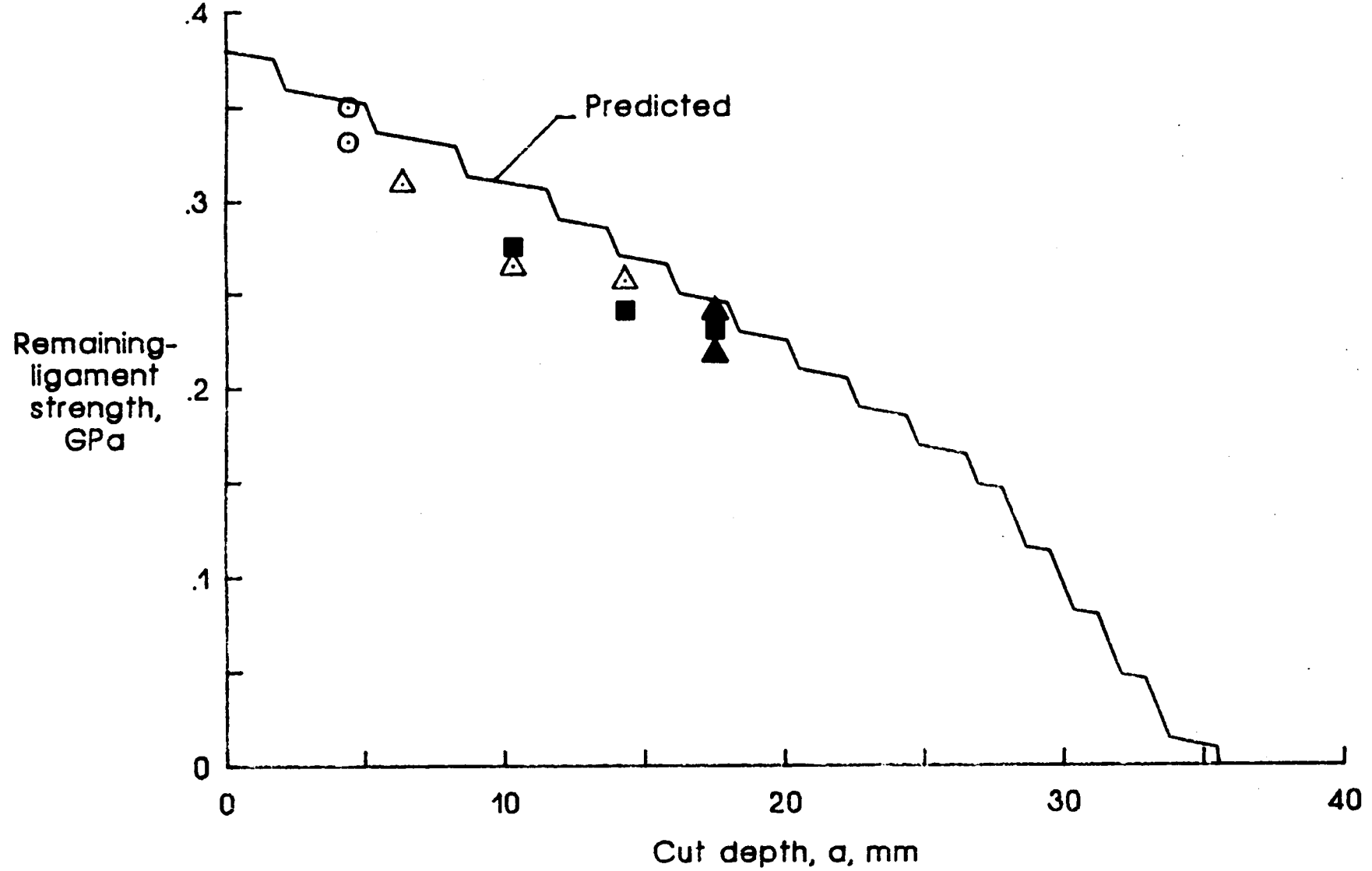

(b) Remaining-ligament strength.

Figure 13.- Concluded.

FIG13B.OMA

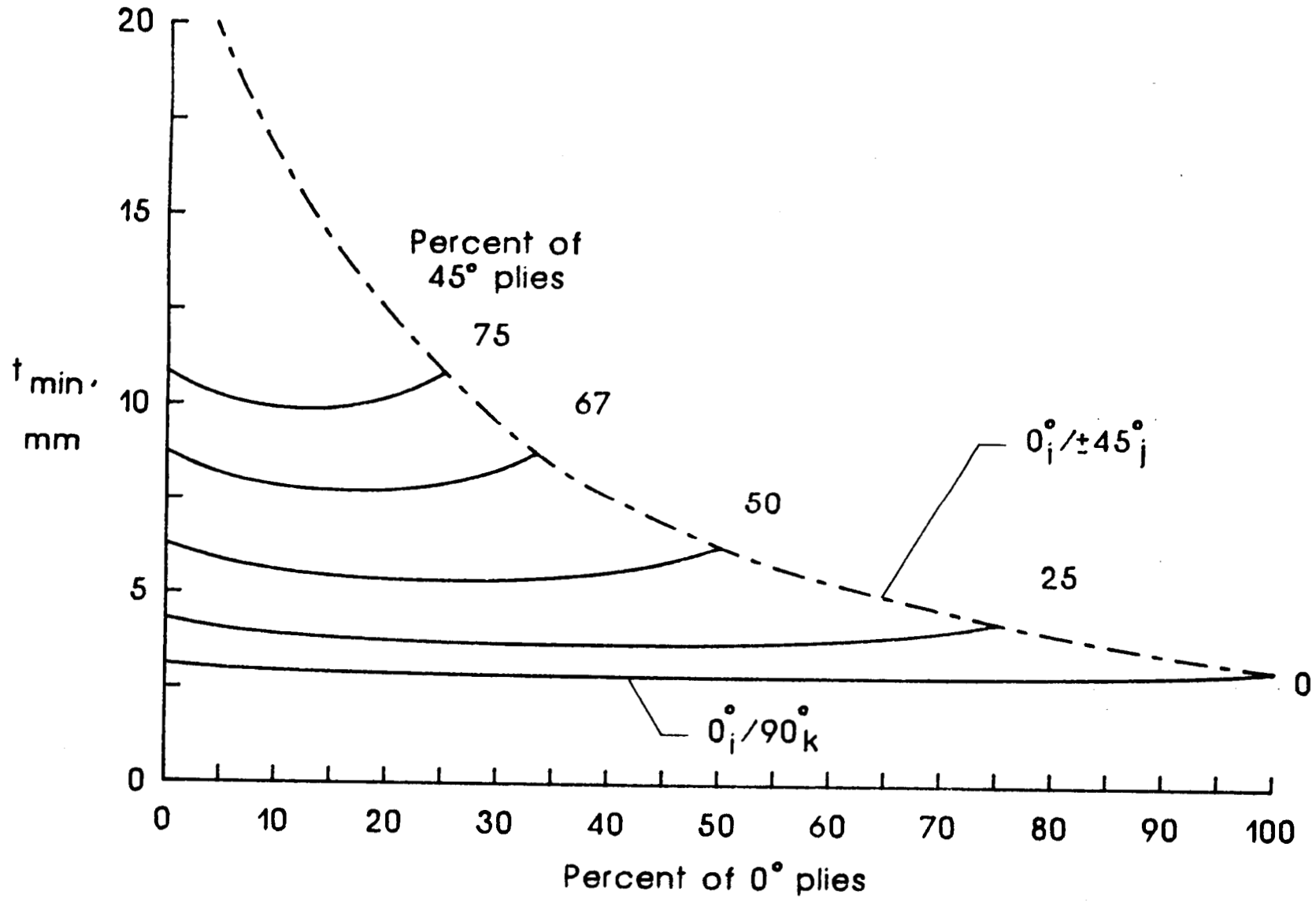

Figure 14.- Predicted minimum thickness of $[0^\circ_i/\pm 45^\circ_j/90^\circ_k]_{ns}$ T300/5208 laminates to result in two-part failure.

PLOT2C.OMA

Standard Bibliographic Page

1. Report No.	2. Government Accession No.	3. Recipient's Catalog No.
NASA TM-89100		

4. Title and Subtitle	5. Report Date
A PARAMETRIC STUDY OF FRACTURE TOUGHNESS OF FIBROUS COMPOSITE MATERIALS	February 1987
	6. Performing Organization Code: 506-43-11-04
7. Author(s): C. C. Poe, Jr.	8. Performing Organization Report No.
9. Performing Organization Name and Address: NASA Langley Research Center, Hampton, VA 23665-5225	10. Work Unit No.
	11. Contract or Grant No.
12. Sponsoring Agency Name and Address: National Aeronautics and Space Administration, Washington, DC 20546	13. Type of Report and Period Covered: Technical Memorandum
	14. Sponsoring Agency Code

15. Supplementary Notes

16. Abstract

Impacts to fibrous composite laminates by objects with low velocities can break fibers giving crack-like damage. The damage may not extend completely through a thick laminate. The tension strength of these damage laminates is reduced much like that of cracked metals. The fracture toughness depends on fiber and matrix properties, fiber orientations, and stacking sequence. Accordingly, a parametric study was made to determine how fiber and matrix properties and fiber orientations affect fracture toughness and notch sensitivity. The values of fracture toughness were predicted from the elastic constants of the laminate and the failing strain of the fibers using a general fracture toughness parameter developed previously. For a variety of laminates, values of fracture toughness from tests of center-cracked specimens and values of residual strength from tests of thick laminates with surface cracks were compared to the predictions to give credibility to the study. In contrast to the usual behavior of metals, it is shown that both ultimate tensile strength and fracture toughness of composites can be increased without increasing notch sensitivity and that laminates with surface cracks can fail in to stages, giving some degree of redundancy.

17. Key Words (Suggested by Authors(s))	18. Distribution Statement
Composite materials Fracture mechanics Fracture toughness Hybrids Surface cracks	Unclassified - Unlimited Subject Category - 24

19. Security Classif.(of this report)	20. Security Classif.(of this page)	21. No. of Pages	22. Price
Unclassified	Unclassified	34	A03

For sale by the National Technical Information Service, Springfield, Virginia 22161